

on the nominal prompt fluxes.

While we are then confident that there is no important contribution to the prompt negative muon flux from muons produced upstream of the target, the small excess of prompt positive muons may result from such backgrounds. While the positive-to-negative ratios, measured to be of the order of 1.20 at the various energies, appear to differ from 1 by more than our estimate of systematic errors would indicate, we do not feel that we have firmly excluded the possibility that the charge asymmetric backgrounds, which we have noted, account for the observed charge differences in the prompt-muon intensities.

Although the ratios determined in these measurements are smaller than the canonical number of 10^{-4} seen at small x and at large transverse momenta, the prompt fluxes—especially at the larger values of x —are still appreciably larger, by about a factor of 5, than we can account for from conventional processes such as vector-meson decay. We note again⁴ that the variation of the

muon-to-pion ratios with x is similar to that which might be expected if the muon were produced by the decay of a parent state (which could be a virtual photon) which is produced with an inclusive spectrum similar to the pion spectrum.

While this work was possible only through the cooperation of the whole of the Fermilab staff, we wish to thank Dr. R. Rubinstein and Dr. C. T. Murphy for their special contribution and encouragement.

¹F. W. Busser *et al.*, Phys. Lett. **53B**, 212 (1974).

²J. P. Boymond *et al.*, Phys. Rev. Lett. **33**, 112 (1974).

³J. A. Appel *et al.*, Phys. Rev. Lett. **33**, 722 (1974).

⁴L. B. Leipuner *et al.*, Phys. Rev. Lett. **34**, 103 (1975).

⁵E. W. Beier *et al.*, in Proceedings of the International Conference on High Energy Physics, Palermo, Italy, 1975 (to be published), Paper B-05.

⁶R. K. Adair, Phys. Rev. Lett. **33**, 115 (1974).

⁷M. G. Albrow *et al.*, Nucl. Phys. **B73**, 40 (1974).

Photoproduction of the $\psi(3100)$ Meson at 11 GeV*

B. Gittelman, K. M. Hanson,† D. Larson, E. Loh,‡ A. Silverman, and G. Theodosiou
Laboratory of Nuclear Studies, Cornell University, Ithaca, New York 14853

(Received 11 August 1975)

The photoproduction of the $\psi(3100)$ meson from a beryllium target has been measured using an 11.8-GeV bremsstrahlung beam. The energy and angular dependence of the measured spectra may be obtained from an elastic nucleon cross section of the form $d\sigma/dt = (1.01 \pm 0.20) \exp[(1.25 \pm 0.20)t]$ nb/GeV². This cross section is exceedingly small in comparison with those of the other vector mesons.

The recently discovered $\psi(3100)$ resonance¹ is believed to be a vector meson. Our picture of the coupling of the other vector mesons to hadronic matter has been strongly influenced by the photoproduction cross sections of these particles. In particular, the cross sections at small momentum transfer are characterized approximately by an energy-independent exponential in the square of the momentum transfer. This simple empirical property has been interpreted as evidence for a diffractivelike production mechanism. Explicit models, such as vector dominance, enable one to calculate the meson-hadron couplings from these cross sections. As a consequence, it is natural to study the photoproduction of the $\psi(3100)$ in order to compare it to the other vector mesons. In this paper we report a measurement of this

cross section for incident photons of energy between 9.0 and 11.8 GeV.

In this experiment a collimated photon beam of 11.8-GeV endpoint energy passes through a 2.9-g/cm² beryllium target, between a set of particle counters, and stops in a secondary-emission quantameter. Energetic photons and electrons leaving the target are detected in a pair of lead-glass Cherenkov hodoscopes. Each hodoscope consists of an 8×10 array of SF-2 glass elements, each 4.5 cm \times 4.5 cm \times 50 cm long, viewed on end by an XP1010 phototube. These hodoscopes have an energy resolution of $\delta E/E = (0.16 \text{ GeV}^{1/2})/\sqrt{E}$, rms, and a position resolution of $\delta s = 0.6$ cm, rms, at 5 GeV. They were placed symmetrically above and below the beam 152.4 cm downstream of the target with their centers

separated vertically from the beam by 48 cm. The glass hodoscopes were calibrated periodically during the course of the experiment with momentum-analyzed positrons. A seven-element scintillation-counter hodoscope was installed directly in front of each glass hodoscope. The scintillators were 5 cm \times 25 cm \times 5 cm thick and were oriented with the 25-cm dimension vertical so that the counting rate variation between them was minimized. A weak magnetic sweep field ($\int B dl = 850$ G m) was used to prevent low-energy charged particles from reaching the scintillation counters.

An event trigger consisted of a coincidence between the two glass hodoscopes for which the energy in each was greater than 2.5 GeV and their sum was greater than 7.0 GeV. For each event, the pulse height of all counters was recorded. In addition, during the last half of the data taking, the time of the scintillation-counter pulse relative to the event-trigger signal was also recorded. The accumulated incident flux was 3.28×10^{15} equivalent quanta taken at an average beam intensity of 2×10^{11} equivalent quanta per minute.

Most events consist of one or two well-isolated, high-energy shower signals in each lead-glass hodoscope and a sprinkling of lower-energy signals distributed elsewhere throughout the hodoscopes. For each hodoscope the position of the center of the most energetic shower and its energy are used to calculate the momentum vector of the detected electron or photon assuming it came from the target. On the basis of the pulse height in the scintillation counter in front of the shower, the detected particle is called charged or neutral. The events are then classified as charged-charged (c-c), neutral-charged (n-c), or neutral-neutral (n-n).

The square of the mass distribution of the two-particle system is shown in Fig. 1 for the three charge states. One notes the bump at $M_x^2 = 9$ GeV² in the c-c spectrum and its absence in the n-c and n-n spectra. The M_x^2 scale of Fig. 1 is that obtained from the on-line energy calibration of the lead-glass counters. Since our results do not depend critically on this calibration, no attempt has been made to refine it. The 542 events in the c-c spectrum with M_x^2 in the range $7.5 < M_x^2 < 11.0$ GeV² constitute our sample of ψ mesons. The background which extends under the ψ peak arises from two sources. The first source comes from the experimental misidentification of photons as charged particles due to either photon conversion or accidentals. The

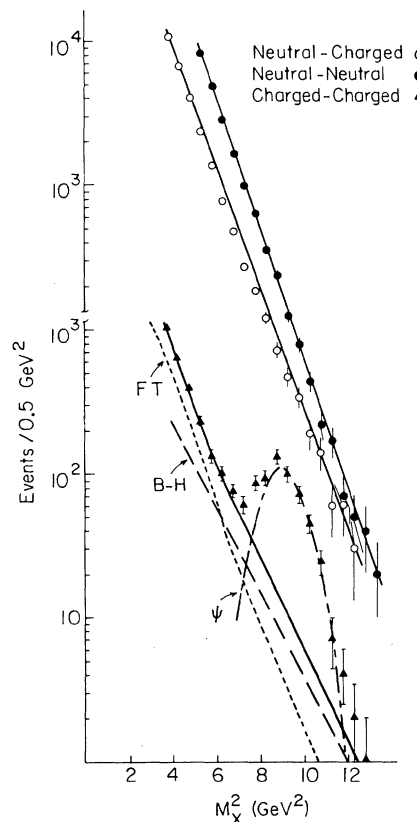


FIG. 1. The two-particle M_x^2 spectra for each of the three charge states. The curves drawn through the n-n and n-c data points are merely to guide the eye. The expected resolution function is drawn through the c-c data points at the ψ mass. The solid line associated with the c-c spectrum is the background arising from Bethe-Heitler pairs (B-H) and experimental feed-through (FT) of n-n and n-c events.

spectrum of these n-n and n-c "feedthroughs" is calculated from the measured n-n and n-c spectra. The second source of background is the normal electromagnetic production of wide-angle electron pairs (i.e., Bethe-Heitler). This contribution is calculated for our experimental situation using the formulas of Tsai² for both elastic and inelastic processes. The measured c-c spectrum in Fig. 1 agrees well with the sum of these backgrounds below 7.5 GeV². The calculated background in the ψ peak region is seventy events.

This explanation of the background is also found to reproduce the $t - t_{\min}$ distribution of the c-c events in the interval $4.4 < M_x^2 < 6.6$ GeV², Fig. 2(b). The $t - t_{\min}$ distribution of the ψ events is displayed in Fig. 2(a). After subtracting the calculated background shown, the data are fitted

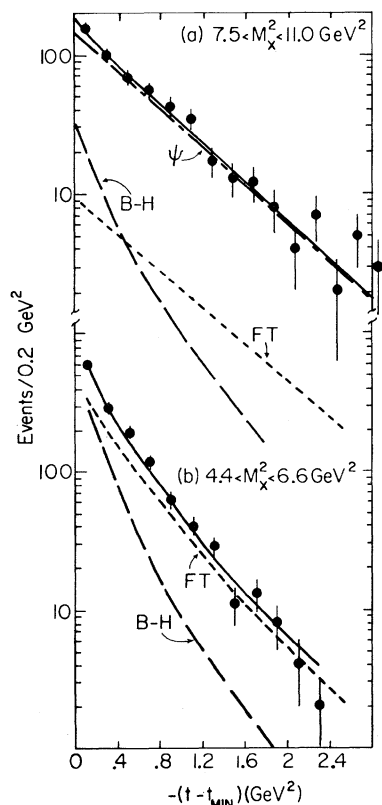


FIG. 2. $t - t_{\min}$ distributions for $c\text{-}c$ events in two mass regions. The solid curves represent the sum of the contributions from Bethe-Heitler pairs (B-H), $n\text{-}n$ and $n\text{-}c$ feedthrough (FT), and for (a) the ψ cross section described in the text.

by a distribution calculated on the basis of a ψ photoproduction cross section of the form $d\sigma/dt = A \exp(bt)$, a bremsstrahlung spectrum, the detector acceptance, and the decay distribution of a spin-1 particle of helicity ± 1 . It is assumed that the production from beryllium is 9 times that from a nucleon (note $t_{\min} = -0.41 \text{ GeV}^2$ at 11 GeV) and the branching ratio for $\psi \rightarrow e^+e^-$ is 0.07. Correction factors for the following experimental effects are included in the normalization: scintillation-counter geometry (1.46 ± 0.04), trigger-logic deadtime (1.04 ± 0.02), beam missing quantummeter (0.998 ± 0.005), loss from scintillation-counter pulse-height cuts (1.16 ± 0.04), loss from M_x^2 cut (1.075 ± 0.025), and radiative corrections (1.043 ± 0.010). The fitted values of A and b are $0.90 \pm 0.10 \text{ nb/GeV}^2$ and $1.13 \pm 0.18 \text{ GeV}^{-2}$.

The incident photon energy for each ψ event can be reconstructed from the measured ψ energy and production angle under the assumption that the ψ 's are elastically produced. If E_t and E_b denote

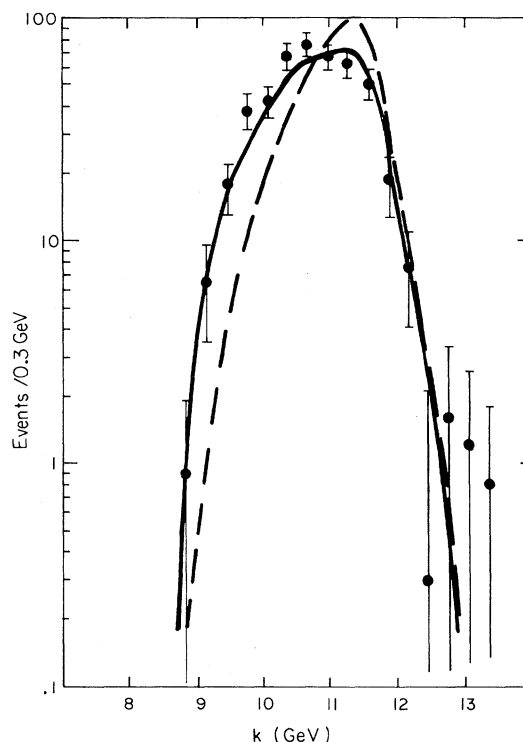


FIG. 3. The reconstructed photon energy distribution for the ψ events with Bethe-Heitler pairs and feed-throughs subtracted. The solid line is the expected distribution for a cross section $d\sigma/dt = 0.9 \exp(1.2t)$. The dashed line is for $d\sigma/dt = 0.144(k - 8.2)^2 \exp(1.2t) \text{ nb/GeV}^2$.

the energies measured in the top and bottom glass counters, the ψ energy written as $E_\psi = E_t + E_b$ has a resolution of 5%, rms. One improves on this resolution if use is made of the measured opening angle, Ω , which has about 0.7% resolution. Assuming the events in the interval $7.5 < m^2 < 11 \text{ GeV}^2$ all have the mass of the ψ , m_ψ , the ψ energy given by

$$E_\psi = (m_\psi / \sin \frac{1}{2} \Omega) (E_t + E_b) / (4E_t E_b)^{1/2}$$

has an accuracy of better than 2% rms for our experimental conditions. The photon energy spectrum obtained for the ψ events, Fig. 3, is in agreement with that expected for a production cross section of the form $A \exp(bt)$. For comparison, the distribution calculated for the case in which A has an energy dependence of the form $A = A_0(k - k_{\text{thres}})^2$, where k_{thres} is the threshold for ψ photoproduction (8.2 GeV), does not follow the data. To analyze the data further, the ψ events are divided into three photon energy in-

tervals, 9.3–10.4–11.1–11.8 GeV. The $t - t_{\min}$ distributions in each interval are fitted by a production cross section of form $A \exp(bt)$ after the calculated backgrounds are removed. The results in the respective energy regions are 0.94 ± 0.20 , 1.10 ± 0.17 , and 0.60 ± 0.12 nb/GeV² for A , and 0.97 ± 0.25 , 1.31 ± 0.19 , and 0.92 ± 0.21 GeV⁻² for b . One may conclude that either the elastic cross section coefficient, A , is independent of energy and there is no statistically significant evidence for inelastic production, or the coefficient has an energy dependence which just compensates the inelastic production so that it appears to be constant.

The effect of the internal motion of the nucleons in the beryllium target nucleus has been studied. Using a phase-space distribution, $f(p)dp = 375 \times p^2 dp$ ($p < 0.2$ GeV/ c), $f(p)dp = 0$ ($p > 0.2$ GeV/ c),³ for the target momentum spectrum, no significant change is found in the calculated $t - t_{\min}$ or k distributions. The fitted values of A and b increase slightly to 1.01 nb/GeV² and 1.25 GeV⁻².

Taking into account the systematic experimental uncertainties as well as the possible inelastic contributions, our value for the elastic cross section parameters becomes $A = 1.01 \pm 0.20$ nb/GeV² and $b = 1.25 \pm 0.20$ GeV⁻² at an energy of 11.0 GeV. There have been two other recent measurements of the photoproduction cross section at somewhat higher energies.^{4,5} These results, together with ours, indicate that the forward cross section, starting above 11.8 GeV, rises rapidly with energy, reaching a value of 20 nb/GeV² at $k = 20$ GeV and 50 nb/GeV² at 100 GeV.⁶ This behavior was qualitatively suggested by Harari⁷ based on arguments relating Zweig's

rule and charm threshold.

The authors wish to thank Professor R. M. Talman, Professor H. Feshbach, and Professor E. J. Moniz for discussions of the problem of internal nucleon motion and Dr. D. Andrews for an independent calculation of the Bethe-Heitler background. We also acknowledge that a large measure of the credit for the success of this experiment is owed to Professor B. D. McDaniel and the technical staff of the Wilson Synchrotron Laboratory.

*Work supported in part by the National Science Foundation.

†Present address: Meson Physics Division, Los Alamos Scientific Laboratory, P. O. Box 1663, Los Alamos, N. M. 87545.

‡Present address: Department of Physics, University of Utah, Salt Lake City, Utah 84112.

¹J. J. Aubert *et al.*, Phys. Rev. Lett. **33**, 1404 (1974); J.-E. Augustin *et al.*, Phys. Rev. Lett. **33**, 1406 (1974).

²Y. S. Tsai, Rev. Mod. Phys. **46**, 815 (1974).

³R. R. Whitney *et al.*, Phys. Rev. C **9**, 2230 (1974).

⁴B. Knapp *et al.*, Phys. Rev. Lett. **34**, 1040 (1975).

⁵U. Camerini *et al.*, Phys. Rev. Lett. **35**, 483 (1975).

⁶Because of the Fermi motion, there is possibly a substantial contribution to the observed rate in our experiment from photons of effective laboratory energy, $k_{eff} = (s - m_p^2)/(2m_p)$, above 13 GeV, where the cross section is measured (Ref. 5) to be almost an order of magnitude larger than our result. The calculation of such a contribution depends critically upon the momentum distribution assumed to describe the Fermi motion as well as the details of the k and t dependence of the cross section above 12 GeV, which are not yet known. This matter is still under study.

⁷H. Harari, informal notes on the nature of the ψ particles [SLAC Report No. SLAC-PUB-1514, 1974 (unpublished)].

Magnetic Moment of the Proton in H₂O in Bohr Magnetons*

William D. Phillips, William E. Cooke, and Daniel Kleppner

Research Laboratory of Electronics and Department of Physics, Massachusetts Institute of Technology, Cambridge, Massachusetts 02139

(Received 13 October 1975)

We have measured the ratio of the magnetic moment of the electron in hydrogen to the magnetic moment of the proton in H₂O to be $g_j(\text{H})/g_p' = 658.216\ 0091(68)$ [10 parts per billion (ppb)], at a temperature of 34.7°C. This yields a value for the proton moment in Bohr magnetons of $\mu_p'/\mu_B = 0.001\ 520\ 992\ 983(17)$ (11 ppb). Our result differs from the currently accepted value by 150 ppb.

Most fundamental experiments in atomic physics which involve determination of a magnetic field yield results in terms of an NMR frequency;

in order to relate the results to useful atomic constants the magnetic moment of the proton as observed under NMR conditions must be known in